Multi-Packet Interference in Opportunistic Large Array Broadcasts over Disk Networks

Haejoon Jung, *Student Member, IEEE,* and Mary Ann Weitnauer*, *Senior Member, IEEE*

***Abstract*—The Opportunistic Large Array (OLA) is a simple form of cooperative transmission, in which a group of single-antenna nodes decode the same packet, then a short time later relay the packet simultaneously in orthogonal or space-time coded channels. The authors have previously shown that OLA transmissions can be adequately synchronized so they appear to a receiver as having come from a conventional array with co-located antennas doing transmit diversity. OLAs have been considered as a basis for rapid single-packet broadcasting in multi-hop networks, however, there are few studies that consider OLA broadcasting of multiple co-channel packets. Using the continuum assumption (approximated by high density networks), we focus on broadcast throughput optimization, as determined by the packet insertion rate at the source. We consider spatial pipelining, which means broadcasting a packet before the previous co-channel packet has cleared the network. We show theoretically that for infinitely large networks the feasibility of spatial pipelining depends on the path loss exponent. For finite networks, we study the propagation behavior of spatially pipelined packets using numerical analysis.**

***Index Terms*—Ad-hoc networks, cooperative diversity, transmit diversity.**

I. Introduction

THE subject of broadcasting in multi-hop wireless networks has attracted the attention of many researchers over the years [1], and there are a number of popular techniques, such as flooding [2], the Probabilistic, Counter, and Location based schemes [3], and broadcast trees [4], [5]. Broadcasts that carry routine vehicle state information and emergency messages have inspired some new broadcast protocols for multi-hop in vehicular ad hoc networks (VANETs) [6], [7]. All of these methods rely on links between a single transmitter and a single receiver.

In contrast, some broadcasting schemes exploit cooperative transmission (CT), in which multiple single-antenna radios gang together to send the same message in independently fading channels so that a receiver can derive a signal-to-noise-ratio (SNR) advantage through diversity combining [8], [9]. This class of schemes include different ways to create diversity channels, such as orthogonal waveforms [10], distributed space-time block codes [11], or phase dithering [12]. Any of these diversity methods can be used with the opportunistic large array (OLA) [13]. An OLA is formed when a group of radios that all decode the same packet next relay that packet at approximately the same time, as a virtual array. In an OLA broadcast, OLAs are formed in succession, as a new group of nodes are able to decode the OLA transmission from the previous group, forming ever-growing ring-shaped OLAs [14]. Practical OLA transmission has been demonstrated by the authors [15]. The OLA broadcasts are known to be fast and reliable, and able to overcome voids that would cause partitions in networks that do non-cooperative transmission [16]. Because no topology information must be stored, OLA broadcasting is especially attractive for highly mobile networks [17]. The OLA broadcast has also been proposed as the route-request step in two reactive OLA-based unicast routing protocols [12], [15], [17], [18].

However, most studies of OLA broadcasts do not consider the interference between co-channel packets in a multi-packet broadcast, such as would occur in the broadcast of a large file. Instead, they consider just a one-shot broadcast of a single packet, which fully utilizes the range extension property of CT. However, if more than just a single packet should be transmitted, for example, if video data needs to be broadcasted over a tactical mobile ad hoc network, then broadcast throughput becomes important. This paper examines the "intra-flow interference" caused by multiple OLAs transmitting different packets from the same source (a single flow) at the same time in different rings of the broadcast. We do not consider "inter-flow interference" that would be caused by broadcasts from different sources.

To our knowledge, only two other research groups have addressed OLA transmissions of multiple packets. The authors of [12] proposed to insert multiple packets into the network with a fixed period as with conventional single-input-single-output (SISO) multi-hop transmissions. They argue that large inter-packet separation can be chosen to trade throughput for enhanced robustness to topological variation, but the impact of the increased intra-flow interference by CT is not investigated in detail. In their recent work in [19], they only consider "inter-flow" interference caused by different flows using protocol interference model, where the interference is assumed to be zero, if the interfering node is outside of a certain range. Because they assume protocol interference model with a constant inter-packet separation, the intra-flow interference from a large number of nodes far from the receiver is not considered.

Manuscript received December 3, 2012; revised May 7, May 21, August 2, and August 23, 2013; accepted September 3, 2013. The associate editor coordinating the review of this paper and approving it for publication was A. Sezgin.

*Mary Ann Weitnauer was formerly Mary Ann Ingram.

The authors are with the Department of Electrical and Computer Engineering, Georgia Institute of Technology, Atlanta, GA, 30332 USA (e-mail: hjung35@gatech.edu, mary.ann.weitnauer@ece.gatech.edu).

The material in this paper was presented in part at the Annual Military Communications Conference (MILCOM), November 2011, Baltimore, MD, USA.

The authors gratefully acknowledge partial support for this research from the National Science Foundation, grant number CNS-1017984.

Digital Object Identifier 10.1109/TWC.2013.093013.121912

Therefore, to our knowledge, only one paper [20], besides our conference version of this paper [21], treats intra-flow interference in OLA broadcasts. [20] assumes perfect interference cancellation of interference from preceding packets, and analyzes the effects of the interference from the following packets. However, for some types of networks such as sensor networks, constraints on node processors and memory may preclude interference cancellation. Also, the presence of multiple time and frequency offsets of cooperators may make channel estimation very challenging [22]. Therefore, we assume that none of the interference is cancelled. Moreover, while the authors in [20] analyze the broadcast capacity from an information theoretical point of view, we focus on the packet-level analysis following [23], in which the inter-packet separation is minimized to maximize the throughput. The conference version of this paper in [21] analyzes the intra-flow interference in OLA broadcasts over disk networks only with the path loss exponent of $\alpha = 2$. In contrast, this paper explores $\alpha \geq 2$, and finds that the path loss exponent α is a key parameter that determines the feasibility as well as the optimal inter-packet spacing. To be specific, the analytical results in this paper show that OLA broadcasting with spatial pipelining is only feasible in the infinitely large disk network for $\alpha > 2$, while $\alpha = 2$ precludes spatial pipelining. This result with $\alpha = 2$ is distinct from the results in [20], which shows constant broadcast capacity can be achieved regardless of $\alpha \geq 2$, because of their interference cancellation assumption.

The organization of the paper is as follows. In Section II, the system model using continuum and deterministic channel assumptions is presented. In Section III, the feasibility of spatially pipelined OLA broadcasts in infinite disk networks is studied with free space path loss exponent of $\alpha = 2$ and higher exponent of $\alpha > 2$, as summarized in Table I, then the impact of the system parameters on the broadcast throughput is theoretically analyzed. In Section IV, numerical results of finite disk networks of $\alpha = 2$ case are presented including step-size control, which is a transmit power adaptation technique. Section V provides the numerically computed optimal broadcast throughput with the given parameters for $\alpha > 2$ in the finite disk network, and presents numerical results showing propagation patterns and relationship of optimal broadcast throughput with different system parameters.

II. System Model

We consider a network with a single source and multiple receivers for the broadcast traffic, where the source broadcasts multiple packets to the other nodes in the network. The wireless nodes except the source are assumed to be the receivers, which are also the decode-and-forward (DF) relay nodes for multi-hop broadcasts. The nodes are assumed to be half-duplex, which means they cannot transmit and receive at the same time. We assume that the source node is in the center of the network, at the origin of a two dimensional plane as indicated by the red square in Fig. 1, while the receiver nodes are uniformly and randomly distributed with average density of ρ. In multi-hop OLA transmissions, when a node receives a packet, it forwards the packet only when the decoding is successful and the node has not transmitted the packet before [13].

As in [14] and [24], let P_s and P_r denote the fixed transmit powers from the source and relay, respectively. For simplicity, we assume the unit noise power as indicated by $\mathbf{N} = 1$ as in [14] and [24], without loss of generality. In this paper, we consider the received signal-to-noise ratio (SNR) in the absence of the interference and the received signal-to-interference-plus-noise ratio (SINR) in the presence of the interference. Therefore, we can apply the results with the unit noise power $\mathbf{N} = 1$ to general cases $\mathbf{N} \neq 1$ by adapting the transmit powers P_s and P_r, accordingly. In other words, the two system parameters P_s and P_r are the transmit powers normalized by the noise or noise plus interference power. Moreover, even in the presence of the interference, the analysis based on the SINR can be generalized in the same manner, because we assume the same transmit power P_r for all the nodes except the source, the transmit power of which is P_s. By the unit noise power assumption, the received power denoted by $\mathbf{S}$ can be used interchangeably with the received signal-to-noise ratio (SNR), which is defined as $\mathbf{S}/\mathbf{N}$. To calculated the received power, when (x, y) is the location of a receiver relative to a transmitter in Cartesian coordinates, for a path loss exponent of α, the path loss function is defined by $l(x, y) = \frac{1}{(x^2+y^2)^{\alpha/2}} = \frac{1}{d^\alpha}$, where $d = (x^2+y^2)^{1/2}$ [14], [24]. In the absence of the interference, the decoding is assumed to be correct if the received SNR is greater than or equal to a certain threshold τ determined by the modulation and coding [14]. A low threshold τ implies a low data rate [24] or a power-efficient waveform such as frequency-shift keying (FSK) [25], because the nodes are required to decode with low received SNR, which means decoding needs to be less demanding. On the other hand, the higher τ implies the higher data rate or bandwidth-efficient waveforms, such as quadrature amplitude modulation (QAM) [25], which require high enough SNR in the absence of the interference (or SINR in the presence of the interference). Therefore, as a minimum requirement for large file transfer applications with bandwidth-efficient waveforms as suggested in [25], we are interested in $\tau \geq 1$, which means the ratio of $\mathbf{S}$ to $\mathbf{N}$ should be greater than or equal to one.

A. Deterministic Channel and Continuum Assumptions

For the multi-hop network analysis with a large number of nodes doing CT, we make the deterministic channel and continuum assumptions, as in [14], [24], [26], [27] and [20], which allows simpler analysis, but is accurate enough for multi-hop OLA transmissions with high node density, as shown in [14] and [24]. In various studies on CT as in [28]–[30], multiple CT transmitters that are physically separated in space are approximated into a single node with multiple-antenna array, which is called *co-located approximation*. However, this co-located approximation causes a significant error especially for the high node density situation as shown in [31] and [32], because this model ignores the disparate path losses from the multiple transmitters to a receiver in a virtual multi-input-single-output (MISO) link of CT.

For this reason, following [14] and [24], we make the "continuum assumption," which is an accurate model of "finite but high" density networks including path-loss disparity in CT

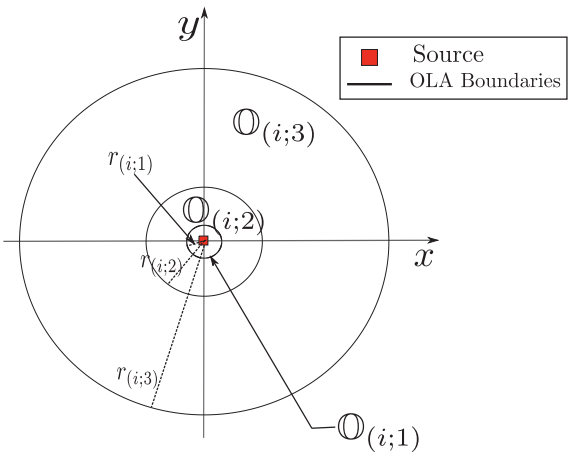

Fig. 1. Coverage analysis based on Continuum approach.

as shown in [14] and [16]. In this continuum model, the node density becomes very large (i.e., $\rho \to \infty$), while the relay transmission per unit area, which is denoted by $\overline{P_r} = \rho P_r$, is held constant. We refer to this particular limit in the sequel as the *"continuum limit."* Also following [14] and [24], we assume the deterministic channel model, which assumes that the power received at a node is the sum of the powers from each of the transmitting nodes. With the two (deterministic channel and continuum) assumptions, the received power from a group of transmitting nodes $\mathbb{O}$, which is originally expressed as $\sum_{j\in\mathbb{O}} P_r \cdot l(d_j)$ by the deterministic channel assumption, can be approximated into an integral form as $\iint_{\mathbb{O}} \overline{P_r} \cdot l(d) dA$, where A is the area of $\mathbb{O}$. Therefore, the SNR at a receiver at a distance z from the origin, receiving power from a disk-shaped OLA of radius r, centered at the origin, such that $r < z$, is $f(r,z) = \int_0^r \int_0^{2\pi} \overline{P_r} \cdot l(r\cos\theta - z, r\sin\theta) r dr d\theta$, where (r,θ) is the transmitter location in polar coordinates.

Since the "sum of powers" property is based on the assumption of every relay transmitting in an orthogonal diversity channel, and in the limit of the continuum, the number of relays goes to infinity, we seem to be assuming infinite bandwidth. However, in practice, only a finite number of orthogonal diversity channels are used, and if these channels are allocated uniformly, then the number of channels is the diversity order. Furthermore, as the diversity order grows, the increase in diversity gain diminishes [33], corresponding to an effective reduction in fading in the SNR after combining. Therefore, our assumptions apply to networks with high node densities and a high number of diversity channels. For example, the authors in [16] show that packet delivery ratio (PDR) of the flat fading channel with a finite node density ($\rho = 2.2$) gets closer to the results based on the "sum of powers" property with the deterministic channel assumption, as they increase the number of diversity channels from one to four. Similarly, in [34], the simulation results of the probability of successful broadcast (PSB) that assumes uniformly and randomly distributed nodes with $\rho = 10$ in Rayleigh fading channel show an excellent match with the analysis based on the deterministic channel assumption, as the number of diversity channels increases from one to three. Moreover, we note that it may be possible to get the same performance with better bandwidth efficiency by using distributed orthogonal space-time codes in [8] instead of orthogonal-frequency or orthogonal-time diversity channels for relays.

It follows from a finite number of diversity channels, that one could assign orthogonal channels for consecutive packets (i.e., simultaneously using different OLAs), which would eliminate the intra-flow interference. However, similarly to the diversity channel allocation to the multiple nodes in an OLA, the number of the channels assigned to the multiple OLAs would be limited in practice. Therefore, if a large file were being broadcasted over a large multi-hop network, channels may need to be reused, in which case, the results in this paper would still apply.

In further support of our system model based on the continuum and deterministic channel assumptions, we note that the simulation results in [16], [24] and the theoretical study in [14] show that the system with cooperative orthogonal transmission has a deterministic SNR by continuum assumption even in the presence of fading and randomness in the channel, which ultimately gives the same result based on the deterministic channel assumption. Therefore, we note that the theoretical and numerical approaches in this paper still work for random fading channels with finite but high node density as well.

B. Validity in Finite-density Networks

In this section, the applicability and limitation of the analytical model based on the two assumptions are described. This paper is focused on how multiple packets propagate in space, the analysis of which is facilitated by the deterministic channel and continuum assumptions. To be specific, we are mainly interested in *packet loss* in multi-packet OLA transmission, which means a packet does not reach the edge of a multi-hop network, for a given inter-packet separation. In the continuum limit, packet loss is indicated in terms of number of hops; that is, a packet is lost if it stops propagating within a finite number of hops (i.e., OLA levels), which is referred to as *transmission die-off* in [14] and [24]. On the other hand, in a real OLA network with finite node density, where the number and placement of nodes are random, packet loss occurs when there is no node that successfully decodes the packet at an intermediate hop before reaching the network edge.

The simulation results in [24], which assume the strip-shaped network, show the propagation prediction based on the continuum assumption is accurate for high enough node density, specifically $\rho = 30$, 50, and 100. For example, when $\rho = 30$, the prediction error in the OLA propagation boundary is less than 2% compared to the simulation results. Moreover, in their disk-shaped network study in [14], the continuum analysis shows less than 5% error of the spatial propagation of OLAs to the simulation results of random and finite-density disk networks, when $\rho = 10$ and 100.

On the other hand, the continuum analysis is not accurate for low node density networks corresponding to $\rho \leq 5$, as shown in the simulation results in [24] and [14]. To be specific, the propagation speed becomes highly random with high standard deviation, as ρ decreases. In particular, for low node-density networks with random fading channel, where the nodes are randomly placed, the packet propagates significantly faster

in some parts of the network, while slower in other areas by the opportunistic feature of OLA. Therefore, in this situation, the OLA propagation pattern becomes irregular depending on the speed in different directions, in contrast to the concentric ring pattern in the continuum limit or high-density network as in [14]. However, we note that because of analytical difficulty to predict this highly random propagation characteristic, this paper is focused on the high-density network with $\rho \geq 10$, where the deterministic channel and continuum assumptions are accurate to model the real network with uniform and random node placement.

C. Single-Packet OLA Broadcast

For the path loss exponent of α, the first OLA for Packet i is a disk denoted $\mathbb{O}_{(i;1)}$, as shown in Fig. 1, with boundary $r_{(i;1)}$, which satisfies ${P_s}/{r_{(i;1)}}^{\alpha} = \tau$, where τ is the decoding threshold. Subsequent OLAs for this packet (Packet i) form concentric rings, centered at the origin. In general, $r_{(i;k-1)}$ and $r_{(i;k)}$ are the inner and outer boundaries, respectively, of Level k OLA $\mathbb{O}_{(i;k)}$ for the same Packet i. We note that the level index k is one less than the index of the hop in which $\mathbb{O}_{(i;k)}$ transmits. For example, for Packet i, the source transmits in the first hop and $\mathbb{O}_{(i;1)}$ transmits in the second hop.

Suppose the receiver location is (z, ϕ) in polar coordinates, where $z > r_{(i;k)}$, at the time that OLA $\mathbb{O}_{(i;k)}$ is transmitting. By circular symmetry, regardless of the angle ϕ, the received SNR at this receiver is denoted $P(\mathbb{O}_{(i;k)} \rightarrow z) = f(r_{(i;k)}, z) - f(r_{(i;k-1)}, z)$, where $f(r,z) = \int_0^r \int_0^{2\pi} \overline{P_r} \cdot l(r\cos\theta - z, r\sin\theta) r dr d\theta$, as defined in the previous section, which does not have a closed form expression except when $\alpha = 2$.

For the free space path attenuation with $\alpha = 2$, the function $f(r,z)$ has a closed form for $z > r$ as shown in [14], which is given by

$$f(r,z)|_{\alpha=2} = \int_0^r \int_0^{2\pi} \frac{r \cdot \overline{P_r}}{r^2 + z^2 - 2rz\cos\theta} dr d\theta = \pi \overline{P_r} \ln \frac{z^2}{|z^2 - r^2|}, \quad (1)$$

where the subscript '$|_{\alpha=2}$' indicates the condition of $\alpha = 2$. Therefore, for $\alpha = 2$, the received SNR $P(\mathbb{O}_{(i;k)} \rightarrow z)|_{\alpha=2}$ can be expressed as

$$\begin{aligned} P(\mathbb{O}_{(i;k)} \rightarrow z)|_{\alpha=2} &= f(r_{(i;k)}, z)|_{\alpha=2} - f(r_{(i;k-1)}, z)|_{\alpha=2} \\ &= \pi \overline{P_r} \left| \ln \frac{z^2}{|z^2 - r_{(i;k)}^2|} - \ln \frac{z^2}{|z^2 - r_{(i-1;k)}^2|} \right| \\ &= \pi \overline{P_r} \left| \ln \frac{\left| z^2 - r_{(i;k-1)}^2 \right|}{\left| z^2 - r_{(i;k)}^2 \right|} \right|, \end{aligned} \quad (2)$$

where the level index $k = 1, 2, 3, \ldots$ and $r_0 = 0$. Also, the absolute value of the logarithm in (10) is just to make sure $P(\mathbb{O}_{(i;k)} \rightarrow z)|_{\alpha=2} \geq 0$.

With this closed form expression assuming $\alpha = 2$, [14] derived the necessary and sufficient condition for the broadcast to the infinite disc network for "free space" attenuation. In the absence of interference, by defining a new variable $\mu = \exp(\frac{\tau}{\pi \overline{P}_r})$, the condition is $\mu = \exp(\frac{\tau}{\pi \overline{P}_r}) \leq 2$ [14].

This condition is interpreted with a physical meaning in [16] using *node degree* $\kappa = \frac{\rho P_r}{\tau}$, which is the average number of nodes in the decoding range of a node. Thus, the condition for $\alpha = 2$ is $\kappa \geq (\ln 2)^{-1}$. In other words, the node degree, which is proportional to the transmit power P_r and node density ρ, should be large enough for the sustained singe-packet OLA broadcasts.

The areas of propagating OLAs are important in the analysis to follow, so we review here the properties of OLA area as a function of hop index in the interference-free case for $\alpha = 2$. To be specific, as proven in [14], the area of Level k OLA, $A_k = \pi[r_{(i;k)}^2 - r_{(i;k-1)}^2]$, which is proportional to the transmitting power of $\mathbb{O}_{(i;k)}$, is given by

$$A_k = \begin{cases} \frac{\pi P_s}{\tau}, & \mu = 2, \\ \frac{\pi P s}{\tau(\mu-1)^{k-1}}, & \mu \neq 2. \end{cases} \quad (3)$$

Therefore, when $\mu < 2$, the areas of the OLA rings A_k grow with the hop index, as illustrated in Fig. 1; we refer to this as the "ring expansion case." As we will show in the following sections, the ring expansion means that an OLA for large k still makes significant interference at the origin. Alternatively, when $\mu = 2$, the area of the OLA is kept equal with different k, because $A_k = P_s/\tau$ for all k. Lastly, if $\mu > 2$, which means that the node degree is not high enough for the sustained single-packet OLA broadcasts (i.e., $\kappa = \frac{\pi \overline{P}_r}{\tau} < \frac{1}{\ln 2}$), the OLA area decreases as k increases. If plugging in $\mu > 2$ in (3), $A_k \rightarrow 0$ as $k \rightarrow \infty$, which means that the single packet will stop propagating after some k. Hence, for the sustained single-packet OLA broadcasts, $\mu \leq 2$ as shown in [14].

In contrast to $\alpha = 2$, when $\alpha > 2$, it is very difficult to obtain a closed form solution of the OLA boundaries, $r_{(i;k)}$. Considering lossy propagation with a higher path loss exponent, $\mu < 2$ is not a sufficient condition but a necessary condition for successful OLA broadcast in the absence of interference (the single-packet case) [35]. Furthermore, there is no notion of κ in the continuum limit as we will now explain. The decoding range of a relay is given by the area inside the circle around the relay with the radius of r_{siso}, where $\frac{P_r}{r_{siso}^{\alpha}} = \tau$. Therefore, in a finite-density network with density ρ, the node degree κ is given by

$$\kappa = \rho \pi r_{siso}^2 = \rho \left(\frac{P_r}{\tau} \right)^{2/\alpha}. \quad (4)$$

We observe that the exponents of ρ and P_r are different, which means κ cannot be expressed as a function of just $\overline{P}_r$, τ and α; therefore, κ is not constant as the continuum limit is approached for $\alpha > 2$. However, we will be able to express bounds in terms of $\overline{P}_r$ in Theorem 3 in Section III-A.

D. Signal Model of Intra-flow Interference

In this section, we consider multiple packets broadcasted from the source to the whole network. We use the definition of the broadcast throughput in [23]: the rate at which packets cross a measurement boundary. In other words, we focus on the packet-level throughput analysis as in [23] assuming the packet size, modulation order, coding ratio or other physical-layer parameters are fixed. In some applications, such as large file broadcast, broadcast throughput is more important than

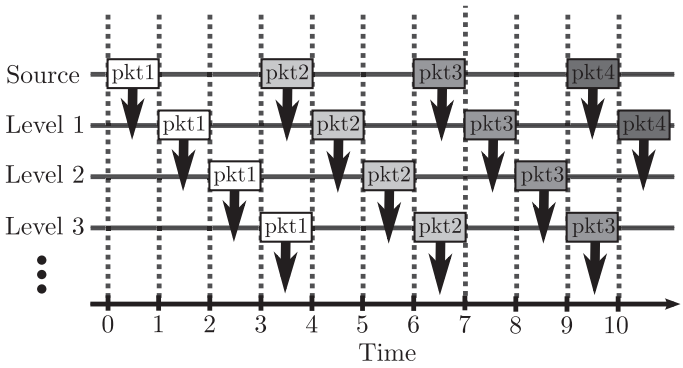

Fig. 2. Timing diagram of spatial pipelined OLA with $M = 3$.

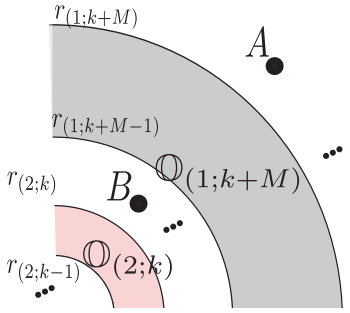

Fig. 3. Intra-flow interference of multiple packets OLA broadcasts.

end-to-end latency of a single packet. If the boundary is at the origin where the source is located, the broadcast throughput is identical to the reciprocal of the packet insertion period at the source (i.e., how often the source can send a new data packet into the network). In the conventional network with single-input-single-output (SISO) links, the packet insertion rate is determined by the time duration that the channel around the source is available again after sending a packet because carrier sense multiple access with collision avoidance (CSMA/CA) is used [36]. However, we note that CSMA/CA, which results in nodes initiating transmission at random times, is not desirable for the OLA transmission, because of the autonomous and distributed control in each node and the need for OLAs to have synchronized transmission. The transmit time synchronization for the same OLA can be achieved based on Global Positioning System (GPS) [12]. Also, in the absence of GPS or other external devices, the preamble-based transmit time synchronization method developed in our research group can be used, as demonstrated using a software-defined radio (SDR) platform in indoor environments in [37]. To be specific, the transmit time synchronization scheme in [37] is designed to support the OLA transmissions. In this scheme, the relays doing CT use an embedded time stamp, which is based on the reception from the previous hop, to hold the packet for a fixed period before firing. The experimental results in [37] show mean rms transmit time spreads on the order of $50ns$ in indoor environments.

Our main interest in this paper is to increase the throughput of OLA broadcasts using *spatial pipelining*, which means broadcasting a co-channel packet before the previous one has cleared the network. We define one time unit as the time duration required for transmission and reception over one hop. Suppose the packet insertion period at the source is M (i.e., the source node injects a new packet into the network every M time units.) Fig. 2 shows an example of spatially pipelined OLA broadcasts with $M = 3$, where the x- and y-axes represent time and OLA level, respectively. In fact, $M = 3$ is the minimum packet insertion period that we can achieve because the nodes are assumed to be half-duplex as defined in Section II. Since $M = 3$ in this example in Fig. 2, the source injects a new packet (from Packet 1 to 4) at $t = 0$, 3, 6, 9 with a fixed period $M = 3$, and the following level OLAs also periodically receive and forward the packets. Therefore, multiple packets, indicated by the squares with different brightness, are propagating across the network at the same time using the same channel with certain inter-separations, which is called *spatial pipelining*.

If the number of transmitted packets is infinite, the broadcast throughput, which is denoted by η, is equal to $1/M$ as long as the decoding conditions for all the packets in the network are satisfied. However, if spatial pipelining causes a critical drop in SINR at the receivers, it is possible for some packets to stop propagating in the middle of the network, which results in lower broadcast throughput. Therefore, we want M to be in the range that no packet loss occurs. On the other hand, we also consider the propagation speed of a packet, which is implied by the hop-distance of the packet. The propagation speed should be positive (non-zero) until the packet reaches the network edge not to stop propagating in the middle of the network.

As a simple example, suppose only two packets are broadcasted such that the second one is transmitted by the source M time slots after the first as shown in Fig.3. The shaded areas in Fig. 3 indicate two OLAs that could be transmitting at the same time. Suppose the smaller one, $\mathbb{O}_{(2;k)}$, transmits the 2nd packet in its $k+1$st hop, and $\mathbb{O}_{(1;k+M)}$, transmits the first packet in its $k+M+1$st hop. We are interested to know if receivers at Points A at radius r_A and B at radius r_B will be able to decode Packets 1 and 2, respectively. We note that $r_{(1;k+M)} < r_A$ and $r_{(2;k)} < r_B < r_{(1;k+M-1)}$.

For the receiver at Point A, we have,

$$\mathbf{SINR}_{(1;k+M+1)}(r_A) = \frac{\mathbf{S}}{\mathbf{I}+\mathbf{N}} = \frac{P(\mathbb{O}_{(1;k+M)} \to r_A)}{P(\mathbb{O}_{(2;k)} \to r_A) + 1}, \tag{5}$$

where $\mathbf{N} = 1$ by the unit noise power assumption. We will assume that if this SINR is greater than τ, the receiver can decode. For the receiver at Point B, the interference comes from the ring, $\mathbb{O}_{(1;k+M)}$, which encloses Point B. We will denote that "backwards propagating" power by $P(r_B \leftarrow \mathbb{O}_{(1;k+M)})$, and for $\alpha = 2$, it can be expressed as

$$P(r_B \leftarrow \mathbb{O}_{(1;k+M)})|_{\alpha=2} = \pi\overline{P_r} \ln\left(\frac{\left|r^2_{(1;k+M)} - r_B^2\right|}{\left|r^2_{(1;k+M-1)} - r_B^2\right|}\right). \tag{6}$$

Thus, for the receiver at Point B, the SINR is

$$\mathbf{SINR}_{(2;k+1)}(r_B) = \frac{P(\mathbb{O}_{(2;k)} \to r_B)}{P\left(r_B \leftarrow \mathbb{O}_{(1;k+M)}\right) + \mathbf{N}}, \tag{7}$$

where $\mathbf{N} = 1$ by the assumption in our system model. Therefore, $r_{(2;k+1)}$ satisfies

$$\mathbf{SINR}_{(2;k+1)}(r_{(2;k+1)}) = \tau. \quad (8)$$

III. Theoretical Analysis of Pipelined Broadcast in the Infinite Disk Network

In this section, we theoretically analyze how the OLA propagation is affected in the infinite disk when multiple packets are transmitted with fixed packet insertion period M (i.e., the Source inserts a new packet every M time units). In particular, we are interested in the feasibility of spatially pipelined OLA broadcasts in the presence of intra-flow interference. This infinite disk network exists only theoretically, but it gives an intuition for very large networks where it takes a large number of hop counts to cover the whole network area. The result is different depending on if the path loss exponent, α, satisfies $\alpha = 2$ or $\alpha > 2$, so we treat these cases in separate sections. To be specific, we will prove that the free space path attenuation with $\alpha = 2$ makes the spatial pipelining infeasible in Section III-A, while the higher path attenuation with $\alpha > 2$ allows multi-packet co-channel OLA transmissions with finite packet insertion period M in Section III-B. Moreover, for the feasible case with path attenuation $\alpha > 2$ we will derive the impacts of two system parameters α and τ on the lower bound of broadcast throughput in Section III-C for the interference-limited case. The final results in this section are summarized in Table I.

A. Feasibility for Free Space Path Loss Exponent ($\alpha = 2$)

In this section, we consider the feasibility of sustained multi-packet OLA broadcasts for $\alpha = 2$. We make the initial assumption that if sustained multi-packet broadcasting for $\alpha = 2$ is possible, then each packet must also at least satisfy the condition for sustained single-packet broadcasting, which is $\mu \leq 2$ [14]. We will show that under this costraint of $\mu \leq 2$, sustained multi-packet broadcasting is infeasible. We will prove this in two parts: first considering the ring expansion case ($\mu < 2$) and second considering the constant-ring-area case ($\mu = 2$). To be specific, for the both cases ($\mu < 2$ and $\mu = 2$), we will show that when $\alpha = 2$, the spatial pipelining is *infeasible* by looking at the SINRs of the two packets (the first and second packets) at the moment the second packet is inserted by the Source M time slots after the first packet was transmitted.

Lemma 1: In the ring expansion case ($\mu < 2$) in the infinitely large network with $\alpha = 2$, the interference from the first packet to a disk around the Source with radius z has a non-zero lower bound regardless of the value of M, when $z \to 0$.

Proof: With the packet insertion gap of M, the interference from the first packet to a receiver at a radius z arbitrarily near the Source is

$$P(z \leftarrow \mathbb{O}_{(1;M-1)})|_{\alpha=2} = \pi\overline{P_r} \ln\left(\frac{\left|r^2_{(1;M-1)} - z^2\right|}{\left|r^2_{(1;M-2)} - z^2\right|}\right), \quad (9)$$

where $r^2_{(1;k)} = \frac{P_s(\mu-1)}{\tau(\mu-2)}\left(1 - \frac{1}{(\mu-1)^k}\right)$ [14]. Therefore, $P(z \leftarrow \mathbb{O}_{(1;M-1)})$ is a decreasing function of M, and an increasing function of z, and has the limit

$$\begin{aligned} P(0 \leftarrow \mathbb{O}_{(1;\infty)})|_{\alpha=2} &= \lim_{z\to 0, M\to\infty} P(z \leftarrow \mathbb{O}_{(1;M-1)})|_{\alpha=2} \\ &= \pi\overline{P_r} \ln\left(\frac{1}{\mu-1}\right) > 0. \end{aligned} \quad (10)$$

■

This implies that no matter how long we wait for the first packet to "move away" from the source, the power from it is never less than $P(0 \leftarrow \mathbb{O}_{(1;\infty)})|_{\alpha=2}$. In other words, the co-channel interference from Packet 1 to Packet 2 at the moment when Packet 2 is inserted does not go to zero, even when $M \to \infty$. The reason is that the OLA widths grow without bound with hop index k. This can be observed by noticing that $r^2_{(1;k+1)} - r^2_{(1;k)}$ is proportional to $1/(\mu-1)^k$.

Lemma 2: For the ring expansion case ($\mu < 2$) in the infinitely large network with $\alpha = 2$, no node at a disk around the Source with radius $z \to 0$ can ever decode the second packet, if

$$P_s < \tau\left[1 + \pi\overline{P_r} \ln\left(\frac{1}{\mu-1}\right)\right]. \quad (11)$$

Proof: The maximum received SNR for Packet 2 is P_s. Therefore, based on Lemma 1, as $M \to \infty$, the maximum SINR at the disk around the source with radius $z \to 0$ is given by

$$\max \mathbf{SINR}_{2;1}(z \to 0)|_{\alpha=2} = \frac{P_s}{1 + \pi\overline{P_r} \ln\left(\frac{1}{\mu-1}\right)}. \quad (12)$$

Hence, if this maximum value is less than the decoding threshold, τ, the second packet cannot form its first OLA, $\mathbb{O}_{(2:1)}$. ■

The feasibility condition of the second packet insertion following (11) in this lemma is because of the ring-expansion of the first packet, which does not experience any co-channel interference until the second packet is inserted. In other words, when Packet 2 is inserted, the Packet 1 has an excessively large OLA, which causes significant interference to Packet 2. This ring expansion is beneficial for the single-packet transmission, because it takes less hops to propagate across the network. However, in the multi-packet OLA transmission, the ring-expansion of Packet 1 suppresses the insertion of Packet 2.

Theorem 1: In the ring expansion case ($\mu < 2$) in the infinitely large network with $\alpha = 2$, when $\tau \geq 1$, the second packet always stops propagating in a finite number of hops. $\tau \geq 1$ corresponds to the class of bandwidth-efficient waveforms [25], which would be desirable for large file transfers.

Proof: Let μ_2 be the version of μ for the interference case. In other words, let $\mu_2 = \exp\left(\frac{\tau(\mathbf{N}+\mathbf{I})}{\pi\overline{P_r}}\right)$. Then, Lemma 2 implies μ_2 has a lower bound,

$$\mu_{2min} = \exp\left(\frac{\tau[1 + P(0 \leftarrow \mathbb{O}_{(1;\infty)})|_{\alpha=2}]}{\pi\overline{P_r}}\right). \quad (13)$$

TABLE I
FEASIBILITY OF SPATIALLY-PIPELINED OLA BROADCASTS IN THE INFINITE DISK NETWORK (α: PATH-LOSS EXPONENT, τ: DECODING THRESHOLD, $\overline{P}_r$: TRANSMIT POWER PER UNIT AREA, $\mu = \exp(\frac{\tau}{\pi \overline{P}_r})$)

Condition		Feasibility	Corresponding Theorem
$\alpha = 2$	$\mu < 2$	Infeasible	Theorem 1 based on Lemmas 1 and 2
	$\mu = 2$	Infeasible for $\tau > 1$	Theorem 2
$\alpha > 2$		Feasible	Theorem 3

By substituting (10),

$$\mu_{2min} = \frac{\mu}{(\mu - 1)^{\tau}}. \tag{14}$$

However, $\frac{\mu}{(\mu-1)^{\tau}} > \frac{\mu}{\mu-1}$ and $\frac{\mu}{\mu-1}$ is a decreasing function of μ over $1 < \mu < 2$. For $\mu = 2$, $\frac{\mu}{\mu-1} = 2$. Thus, $\mu_{2min} > 2$, when $\tau \geq 1$. Therefore, the second packet always stops propagating in finite hops, because the condition for infinite broadcast fails. ∎

Theorem 1 shows that the "ring expansion" property of the OLA broadcasts makes pipelined packet transmission impossible for $\tau \geq 1$. In other words, even if the source transmission power P_s is large enough to insert Packet 2, which means $P_s > \tau[1 + \pi \overline{P_r} \ln\left(\frac{1}{\mu-1}\right)]$ as the opposite case of Lemma 2, Packet 2 always stops propagating for $\tau > 1$, because of the excessive interference from Packet 1, the OLA size of which increases exponentially until Packet 2 is inserted.

One might think that when $\mu = 2$, the pipelined packet transmission is feasible without the packet loss because the limit in (10) goes to zero by plugging the OLA boundary equation in [14], $r^2_{(1;k)} = \frac{P_s k}{\tau}$ into (9). However, this limit $P(0 \leftarrow \mathbb{O}_{(1;\infty)})|_{\alpha=2} \to 0$ holds only when $M \to \infty$, which implies the insertion of Packet 2 should wait for an infinite time after Packet 1 transmission. Also, the following theorem shows that the finite packet insertion rate is not achievable, when $\mu = 2$.

Theorem 2: If $\mu = 2$, $\alpha = 2$, and $\tau \geq 1$, the pipelined packet transmission is impossible in the infinitely large network with a finite M.

Proof: This can be proved by contradiction with the two-packet case as follows. Suppose two packets are successfully broadcasted. By the assumption, $\mu = 2$. We do not allow the transmit power $\overline{P}_r$ to change between packets, so if $\mu = 2$, then $\mu_2 = 2$.

However, a finite packet insertion gap results in $P(0 \leftarrow \mathbb{O}_{(1;M-1)})|_{\alpha=2} = \epsilon$, where ϵ is infinitesimally small positive value. Because 2 is the upper bound of μ for the infinite OLA broadcast, even an infinitesimally small decrease in SINR by $\epsilon(> 0)$ makes μ greater than the upper bound

$$\mu_2 = \exp\left(\frac{\tau(\mathbf{N} + \mathbf{I})}{\pi \overline{P_r}}\right) = \mu^{(1+\epsilon)} > \mu = 2. \tag{15}$$

Hence, the supposition is false, which implies at least one of the two packets stops propagating. Therefore, when $\mu = 2$, the pipelined transmission with a finite M is impossible, too, when $\tau \geq 1$. ∎

Even though $\mu = 2$ does not cause the ring-expansion of Packet 1, spatial pipelining is infeasible, because $\mu = 2$ is the very boundary value for the sustained OLA transmission for the "*single-packet case*." Therefore, if co-channel interference is present, the successful OLA transmission condition in terms of SINR ceases to hold even with extremely small interference. In conclusion, Theorems 1 and 2 show that spatial pipelining of OLA broadcasts in the infinite disk network is infeasible with fixed relay transmission power for the free space path loss exponent $\alpha = 2$.

B. Feasibility for Higher Path Loss Exponent ($\alpha > 2$)

Because many indoor and short-range wireless networks are lossy with higher path loss exponents, we analyze the feasibility of multiple packet OLA broadcasts in infinite networks for $\alpha > 2$ in this section. While $\alpha = 2$ gives a closed form solution of the integral $f(r, z) = \int_0^r \int_0^{2\pi} \overline{P_r} \cdot l(r\cos\theta - z, r\sin\theta) r dr d\theta$, where $l(x, y) = \frac{1}{(x^2+y^2)^{\alpha/2}}$, a closed form solution for $\alpha > 2$ appears to be very difficult to obtain [35]. Therefore, we are not able to derive the closed form expressions of the OLA boundaries even for the single-packet OLA broadcasts. However, [20] shows a sufficient condition of multiple packet OLA broadcast to reach an infinitely large network, propagating at least linearly (i.e., $r_{(i;k)} - r_{(i;k-1)} = \Delta$, where Δ is a positive constant) in the presence of co-channel intra-flow interference from later packets. Even though [20] does not consider the interference from the preceding packets because they assume perfect interference cancellation, their theoretical approach to prove the feasibility of spatial pipelining is still applicable for the interference scenario by modification. In the following theorem, we consider the upper bound of the broadcast throughput for $\alpha > 2$ by introducing the packet insertion period concept, assuming at-least-linearly propagating OLA broadcasts.

Theorem 3: When $\alpha > 2$, it is "feasible" for spatially pipelined packets to propagate over the infinitely large network with at-least-linearly increasing radial distances (the outer boundaries) with a finite $M > 3$ assuming the half-duplex nodes, thereby avoiding any packet loss in infinitely large disk networks.

Proof: Suppose co-channel packets are inserted with packet insertion period of M. In Fig. 4, simultaneous OLAs are indicated by the gray areas. We note that the OLAs are actually concentric rings, however, only partial areas of the OLAs are shown in the illustration. In the figure, the dark-gray area means the desired signal source $\mathbb{O}_{(i;k)}$, while the light-gray areas are the co-channel interfering OLAs, which are infinitely many in the infinite disk network. Also, the dotted line indicates a circle with a radius of $r_{(i;k)} + \Delta$, where $\Delta > 0$, and Point z is on the circle. The semicircle $(C1)$ in Fig. 4, the radius of which is Δ, is centered at the point that is 2Δ away from Point z on the same x-axis. Moreover, the circle

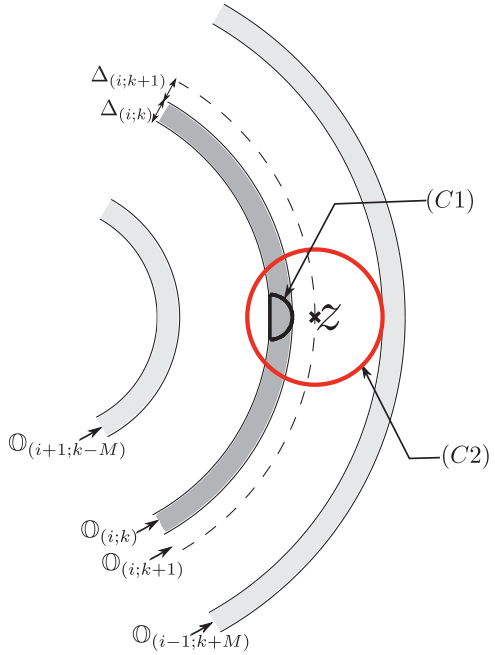

Fig. 4. Illustration to derive the lower bound of SINR for a given packet insertion period M.

$(C2)$, the radius of which is 3Δ, is centered at the point that is Δ away from Point z. To be at-least-linearly propagating, the OLA should have boundaries that satisfy

$$r_{(i;k+1)} \geq r_{(i;k)} + \Delta. \tag{16}$$

In other words, the SINR at Point z must be greater than or equal to the decoding threshold τ for at linearly increasing OLA boundaries.

First, the received signal power $\mathbf{S}$ at Point z has a lower bound $\mathbf{S}_{LB}$ as given by

$$\begin{aligned} \mathbf{S} &= P(\mathbb{O}_{(i;k)} \to z) \\ &> \text{[received power from area inside } (C1)] \\ &\geq \frac{Area(C1)\overline{P}_r}{(2\Delta)^{\alpha}} = \frac{\pi \overline{P}_r}{2^{\alpha+1}\Delta^{\alpha-2}} = \mathbf{S}_{LB}. \end{aligned} \tag{17}$$

On the other hand, the upper bound for the interference $\mathbf{I}_{UB}$ from infinite number of the co-channel packets with packet insertion period of M can be given by

$$\begin{aligned} \mathbf{I} &= \sum_{j\neq 0} P(\mathbb{O}_{(i+j;k-Mj)} \to z) \\ &< \text{[received power from area outside } (C2)] \\ &\overset{(a)}{=} \int_0^{2\pi} \int_{(M-2)\Delta}^{\infty} \overline{P}_r r \cdot l(r) d\theta dr \\ &= \frac{2\pi \overline{P}_r}{(\alpha-2)(M-2)^{\alpha-2}\Delta^{\alpha-2}} = \mathbf{I}_{UB}, \end{aligned} \tag{18}$$

where the domain of the integration at (a) corresponds to the minimum distance from Point z to the closest co-channel OLA assuming linear propagation, which is $(M-2)\Delta$ for $M \geq 3$ as the worst case in terms of SINR. Moreover, we note that this upper bound is also highly inflated compared to the actual co-channel interference, because the domain of the integration is the whole network (to infinity) outside of the region in $(C2)$.

It is feasible for spatially pipelined co-channel packets to propagate at least linearly, when the SINR at Point z is greater than or equal to τ, which is guaranteed when the lower bound $\mathbf{SINR}_{LB}$ is greater than τ as

$$\mathbf{SINR}_{LB} = \frac{\mathbf{S}_{LB}}{\mathbf{I}_{UB} + \mathbf{N}} = \frac{\mathbf{S}_{LB}}{\mathbf{I}_{UB} + 1} \geq \tau, \tag{19}$$

where $\mathbf{S}_{LB} = \frac{\pi \overline{P}_r}{2^{\alpha+1}\Delta^{\alpha-2}}$ and $\mathbf{I}_{UB} = \frac{2\pi \overline{P}_r}{(\alpha-2)(M-2)^{\alpha-2}\Delta^{\alpha-2}}$ represent the lower bound of $\mathbf{S}$ and the upper bound of $\mathbf{I}$ in (17) and (18), respectively. Also, $\mathbf{N} = 1$ by the assumption in Section II. If there is a solution pair (M, Δ), where $M \geq 3$ and $\Delta > 0$, the spatial pipelining of OLA broadcasts is possible without causing any packet loss in infinite disk networks, since all the packets propagate at least linearly across infinite disk networks by Δ. Because $\mathbf{SINR}_{LB}$ is a monotonically increasing function of M, there exist an infinite number of solutions M for a finite τ and given value of Δ, as long as the relay transmission power $\overline{P}_r$ is large enough (it should at least pass the SNR threshold in the absence of interference). ■

The previous theorem treats the kth hop of the ith packet, where $k \geq 1$. When a new packet is inserted at the source, which corresponds to $k = 0$, the only difference with the SINR lower bound for $k \geq 1$ is that the received signal power $\mathbf{S} = P_s/\Delta^{\alpha}$, while the interference term $\mathbf{I}$ has the same upper bound as (18). Therefore, if the source transmission power P_s is high enough, the consecutive packet insertion at the source is feasible, satisfying the linear propagation condition. This feasibility of spatial pipelining for $\alpha > 2$ is because the high path attenuation of the co-channel interference with $\alpha > 2$ is beneficial to enhance the spatial reuse, even though the desired signal component also experiences higher attenuation than $\alpha = 2$. Because the spatial pipelining is feasible in the presence of co-channel interference when $\alpha > 2$, while it is not feasible with $\alpha = 2$, now we need to consider the broadcast throughput optimization. Thus, in the following section, we derive the lower bound of the broadcast throughput using the SINR lower bound in (19).

C. Lower Bound of Broadcast Throughput with $\alpha > 2$ for the Interference-limited Case

In this section, we focus on the theoretical lower bound of the broadcast throughput in the infinite disk network simplifying (19) for the *"interference-limited case"*, by assuming high transmit powers. The key issue in the pipelined OLA broadcasts is the selection of M; we want to find the smallest M satisfying the SINR condition for the infinite disk network that avoids all packet loss, so the throughput $\eta = 1/M$ is maximized. In other words, $M_{I,opt}$ is the minimum packet insertion period M for given parameters such as α, $\overline{P}_r$, τ, with which the spatially pipelined OLA broadcasting has no packet loss in the infinite disk network.

Suppose $\hat{M}_{I,opt} = 1/\hat{\eta}_{I,opt}$ is the solution of (19), then $\hat{\eta}_{I,opt}$ serves as a lower bound of the true optimum $\eta_{I,opt} = 1/M_{I,opt}$, because (19) involves $\mathbf{SINR}_{LB}$, a lower-than-actual SINR. However, it is difficult to solve (19) to obtain $\hat{\eta}_{I,opt} = 1/\hat{M}_{I,opt}$, because of the noise term in the denominator. Hence, in the following Section III-C1, we

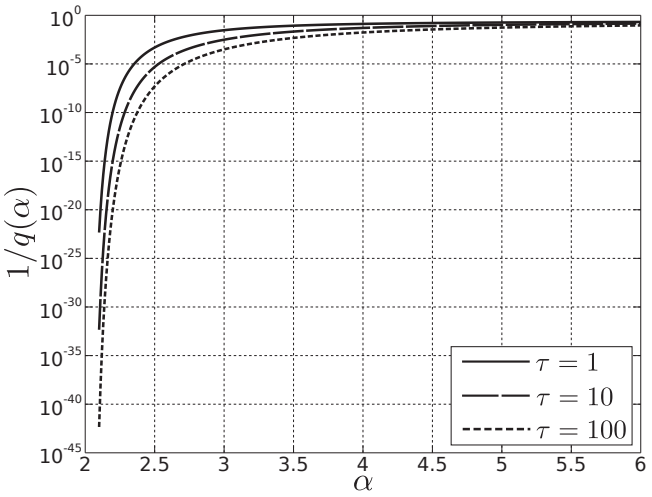

Fig. 5. α versus $1/q(\alpha)$, when $\tau = \{1, 10, 100\}$.

will derive an approximate lower bound $\hat{\eta}^*_{I,opt} = \hat{\eta}_{I,opt}$ in the interference-limited case. Next, we will consider how this bound is impacted by α and τ, in Sections III-C2 and III-C3, respectively. The theoretical results on the impacts of α and τ will be compared with the numeral results in the finite disk network for $\alpha > 2$ in Section V. Lastly, the numerical results in Section III-C4 will show the comparison between $\hat{M}_{I,opt}$ and $\hat{M}^*_{I,opt}$, where $\hat{M}^*_{I,opt}$ is the approximate version of $\hat{M}_{I,opt}$ in the interference-limited case.

1) Approximate Lower Bound $\hat{\eta}^*_{I,opt} = 1/\hat{M}^*_{I,opt}$ for the Interference-limited Case: As $\overline{P}_r \to \infty$, $\mathbf{SINR}_{LB}$ in (19) becomes

$$\mathbf{SINR}_{LB} \approx \mathbf{SIR}_{LB} = \frac{(\alpha-2)(M-2)^{\alpha-2}}{2^{\alpha+2}}. \tag{20}$$

If we solve $\mathbf{SIR}_{LB} \geq \tau$ in terms of M, it gives the minimum packet insertion period as

$$\hat{M}^*_{I,opt} = 2 + \left\lceil \left(\frac{\tau \cdot 2^{\alpha+2}}{\alpha-2} \right)^{\frac{1}{\alpha-2}} \right\rceil, \tag{21}$$

where the ceiling makes $\hat{M}^*_{I,opt}$ a positive integer. This bound is a function of just two parameters: τ and α, so it is easier to find this $\hat{M}^*_{I,opt}$ than $\hat{M}_{I,opt}$ that is the minimum M satisfying (19). Using this approximation, we can find the relationship between the achievable broadcast throughput and the system parameters such as α and τ for the interference-limited regime. The two following subsections show the impacts of α and τ, respectively.

2) $\hat{M}^*_{I,opt}$ and α: Using (21), we can identify the impact of the path loss exponent α on $\hat{M}^*_{I,opt}$ for the interference-limited regime. For simplicity, excluding the ceiling on the right hand side in (21), we define a function $q(\alpha) = 2 + \left(\frac{\tau \cdot 2^{\alpha+2}}{\alpha-2}\right)^{\frac{1}{\alpha-2}}$, which is less than or equal to the original term with the ceiling. If we differentiate $q(\alpha)$ with respect to α, we have

$$q'(\alpha) := \frac{\partial q}{\partial \alpha} = \left(\frac{2^{\alpha+2}\tau}{\alpha-2}\right)^{\frac{1}{\alpha-2}} \times \left(\frac{2^{-\alpha-2}\left(\frac{2^{\alpha+2}\tau \ln 2}{\alpha-2} - \frac{2^{\alpha+2}\tau}{(\alpha-2)^2}\right)}{\tau} - \frac{\ln\left(\frac{2^{\alpha+2}\tau}{\alpha-2}\right)}{(\alpha-2)^2} \right), \tag{22}$$

where $\alpha > 2$ and the solution of $q'(\alpha) = 0$ is $\alpha^* = 2(1+8e^{\tau})$. From the second derivative, $q''(\alpha) = \frac{\partial^2 q}{\partial \alpha^2}$, we have that $q''(\alpha^*) > 0$ for $\tau > 0$. Therefore, the function $q(\alpha)$ is minimized at $\alpha^* = 2(1+8e^{\tau})$. Moreover, because $q'(\alpha) < 0$ for $1 < \alpha < \alpha^*$, q is decreasing as α increases. Hence, in this range the achievable throughput is increasing as α increases. With the ceiling as in (21), $\hat{M}^*_{I,opt}$ is decreasing or kept to be the same, as α increases.

Therefore, for the interference-limited regime, $\hat{\eta}^*{}_{I,opt} = 1/\hat{M}^*_{I,opt}$ is increasing as α increases in the range of $1 < \alpha \leq 2(1+8e^{\tau})$ for the given decoding threshold τ. For the practical interpretation, we assume $\tau \geq 1$, which corresponds to the class of bandwidth-efficient waveforms [25] and appropriate for large file transfers. For example, $\alpha^* \approx 45.4925$ for $\tau = 1$. Therefore, in the practical ranges of τ and α, the lower bound of the broadcast throughput $\hat{\eta}^*_{I,opt}$ increases, as α increases, which implies the better spatial reuse for higher α. This relationship can be observed in Fig. 5, where the horizontal axis represents the path loss exponent α with the practical range $2 < \alpha < 6$ in linear scale, and the vertical axis indicates $1/q(\alpha)$, which satisfies $\hat{\eta}^*{}_{I,opt} = \lfloor 1/q(\alpha) \rfloor$, in log scale. In the figure, the curve with the solid line indicates $1/q(\alpha)$ with $\tau = 1$, while the dashed and dotted curves correspond to the graphs of $1/q(\alpha)$, when $\tau = 10$ and 100, respectively. As shown in the figure, as α increases, all the three curves increase, which confirms our analysis.

3) $\hat{M}^*_{I,opt}$ and τ: Based on (21), we can find that $\hat{\eta}^*_{I,opt}$ decreases as τ increases for the interference-limited case. To prove this, we need to show $\hat{M}^*_{I,opt}$ is increasing when τ increases. Hence, if we differentiate q, which is defined in the previous subsection, with respect to τ, it gives $\frac{\partial q}{\partial \tau}$ as

$$\frac{\partial q}{\partial \tau} = \frac{2^{\alpha+2}\left(\frac{2^{\alpha+2}\tau}{\alpha-2}\right)^{-1+\frac{1}{\alpha-2}}}{(\alpha-2)^2}, \tag{23}$$

which is always positive for $\tau > 0$ and $\alpha > 2$. Therefore, q is a increasing function of τ, and $\hat{M}^*_{I,opt}$,which is equal to ceiling of q, is increasing or kept to be the same (by the ceiling), as τ increases. This behavior is also shown in Fig. 5, where the heights of the curves indicating $1/q(\alpha)$, decrease, as τ increases. Therefore, as τ increases, the corresponding broadcast throughput $\hat{\eta}^*{}_{I,opt} = \lfloor 1/q(\alpha) \rfloor$ decreases.

4) Comparison with Numerical Results: Table II compares the bound, $\hat{M}_{I,opt}$, which corresponds to the *original* lower bound of the broadcast throughput using (19), with the asymptotic bound, $\hat{M}^*_{I,opt}$, in (20) assuming the interference-limited case. In the table, the four rows correspond to α =2.5, 3, 3.5, and 4, while the first four columns represent $\overline{P}_r$ =3, 30, 300, and 3000, and the last column corresponds to $\hat{M}^*_{I,opt}$ for the interference-limited case, when $\tau = 1$. The numerical results in the table show that $\hat{M}_{I,opt}$ decreases as α increases,

TABLE II
NUMERICALLY COMPUTED MINIMUM PACKET INSERTION PERIODS $\hat{M}_{I,opt}$ AND $\hat{M}^*_{I,opt}$ FOR $\tau = 1$

	P_r				
α	3	30	300	3000	$\hat{M}^*_{I,opt}$
2.5	89615	2448	2086	2054	2050
3	214	37	35	35	34
3.5	37	13	12	12	12
4	17	8	8	8	8

which gives higher lower bounds of the broadcast throughputs $\hat{\eta}_{I,opt}$. It is because more efficient spatial reuse is possible by the reduced co-channel interference level with the higher path loss exponent as shown in Section III-C2. On the other hand, the larger $\overline{P}_r$ also results in the decrease of $\hat{M}_{I,opt}$, since $\mathbf{S}_{LB}$ increases relatively more than $\mathbf{I}_{UB}$ by their relative distance gap of the signal source and interfering OLAs. Moreover, $\hat{M}^*_{I,opt}$ based on the SIR instead of the SINR is very close to $\hat{M}_{I,opt}$ when $\overline{P}_r = 3000$. However, because the noise is ignored, it always holds that $\hat{M}^*_{I,opt} \leq \hat{M}_{I,opt}$.

Moreover, the analysis about the impacts of α and τ on the broadcast throughput can be applied to the finite but large enough disk networks, where it takes a large number of hops to reach the network edge as long as the interference dominates the noise power. Also, we will observe the identical trends in the effects of α and τ in the numerical results in Sections V-B and V-C.

IV. NUMERICAL RESULTS WITH THE FINITE DISK NETWORK IN FREE SPACE ($\alpha = 2$)

In this section, we studies whether the broadcast throughput in finite networks can be improved by spatial pipelining with the free space path attenuation (i.e., $\alpha = 2$) by numerical results. To be specific, by using ten-packet examples, where the ten packets are spatially pipelined using the same channel, we will show that when $\alpha = 2$ the spatial pipelining always degrades the broadcast throughputs both for the ring-expansion (i.e., $\mu < 2$) and constant-area-OLA cases (i.e., $\mu = 2$). In a finite network, the interference from the preceding packet to the following packet does not last forever, because there is no more cooperative forwarding of the preceding packet after it reaches the edge of the network. For example, suppose the OLA broadcasts of a single packet take exactly M_0 hops to reach the edge of the network of radius R. The radius of the disk network R satisfies $R^2 = P_s M_0/\tau$ when $\mu = 2$, and $R^2 = \frac{P_s(\mu-1)}{\tau(\mu-2)}\left(1 - \frac{1}{(\mu-1)^{M_0}}\right)$ when $\mu < 2$ [14]. In this case, if we send multiple packets "without" pipelining, the OLA broadcast of each packet will take M_0 time units, so the broadcast throughput $\eta = 1/M_0$ because the minimum packet insertion period M without causing intra-flow interference is M_0

On the other hand, if Packet 2 is inserted $M = M_0 - l$ time slots after Packet 1, where $1 \leq l < M_0$, the receivers of Packet 2 would experience interference from the first packet just for the first l time units, and the packet would propagate without the interference until the third packet comes into the network. The question is whether we can use this interference-free time and do broadcast pipelining, to ultimately improve the broadcast throughput η, which is defined by $1/M$ for the no packet loss case. However, even in this case, when $\alpha = 2$, we will show that pipelined OLA broadcasting does not improve the network throughput because the following packet hop-distances become shorter, which finally causes the packet loss. We will show examples using that the packet loss always occurs with ten packets for $\alpha = 2$. In particular, spatial pipelining can be used with $3 \leq M \leq M_0 - 1$. In this range, the intra-flow interference increases as M decreases, because smaller M means the shorter inter-packet distances. To maximize the broadcast throughput η, we need to find the minimum $M_{R,opt}$ that does not cause any packet loss.

Therefore, as the minimum requirement for the feasibility of spatially pipelined OLA broadcasts, $M = M_0 - 1$ should not cause packet loss for the spatial pipelining. In this case, we insert the second packet at $t = M_0 - 1$, so the two packets coexist on the network, and interfere with each other, for just one time slot (in fact, it can be a little more than one time slot, when the first packet becomes slower by the second packet). The intra-flow interference during this one time unit overlap changes the last (M_0th) hop-distance of the first packet, and also shortens the first hop-distance of the second packet. In particular, the outer boundary of the second packet is the r satisfying $\mathbf{SINR}_{(2;1)}(r) = \frac{P_s/r^2}{1+P(r \leftarrow \mathbb{O}_{(1;M-1)})} = \tau$. Therefore, the initial step of the second packet is smaller than the initial step of the first packet. The small size of the first OLA has a lasting effect; all the second-packet OLA boundary radii will be smaller than their first-packet counterparts. Therefore, the second packet takes at least one more hop than M_0 to reach the edge. Furthermore, the third packet inserted at $t = 2M_0 - 2$ will hurt the radial hop-distance of the second packet, too.

The following numerical results show the effects of this co-channel interference with ten packets. However, because the distances between the packets or OLA step sizes can be an arbitrarily small positive number, the path loss function simply defined by $l(d) = 1/d^\alpha$ does not hold for very small d [38]. As in [14], for the numerical evaluations in this paper, we separate the path loss function depending on d to avoid unrealistically inflated received power, which is given by

$$l(d) \triangleq \begin{cases} 1/d^\alpha, & d \geq 1, \\ 1, & d < 1. \end{cases}, \tag{24}$$

where d is the normalized distance by d_0.

A. Ten-Packet Example

In this section, we show the numerical results of the OLA broadcast with ten packets for $P_s = 10$ and $\tau = 1$ using a pair of graphs. Fig. 6 belongs to the ring expansion case with $\mu = 1.8$ and the radius of the network $R = 300$. In the figure displays the traces of all the 10 packets on the graph of time versus distance, where the horizontal axis is the time and the vertical axis represents the radial distance (from the source to the edge of the network R). Also, each curve indicates the propagation pattern of each packet ($r_{(i;k)}$, where the packet index i is from one to ten), on which the number with the bold font is the final hop count determined either by i) the packet reaches the edge of the network or ii) the packet quits propagating in the middle of the network.

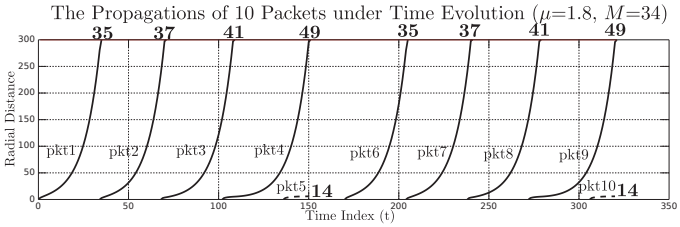

Fig. 6. The time evolution of the distances, when μ=1.8, M=34, M_0=35, and R=300.

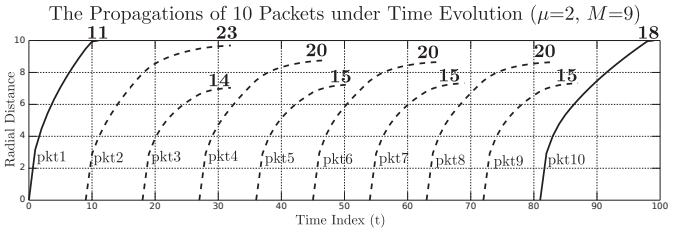

Fig. 7. The time evolution of the distances, when μ=2, M=9, M_0=10, and R=10.

With the given parameters, the single-packet OLA broadcasts take 35 hops to reach the edge of the network, which means $M_0 = 35$. If we use the packet insertion period $M = 35$, all the ten packets propagate identically with the final hop count of 35 because there is no intra-flow interference. On the other hand, the packet insertion period M in Fig. 6 is $34 = M_0 - 1$, which is the marginal value for the spatial pipelining.

Fig. 6 shows that from the second to the fourth packets, the hop counts increase because the lagging second packet interferes with the third more than the first packet interference with the second. The effect sequentially causes more severe reductions in the hop-distances of the packets, until the fifth packet is lost; however, after that, the same pattern is repeated by the next five packets (from six to ten). The slopes of the first to fourth packets are decreasing as the packet index increases, and finally the fifth packet is killed. It is a surprising result in that shortening the packet insertion period by just one slot, to $M = M_0 - 1$, makes multiple-packet pipelining impossible to achieve (i.e., the packet loss is not avoidable).

Fig. 7 shows the case of $\mu = 2$, which does not have the ring expansion property. Because the relay power corresponding to $\mu = 2$ is much lower than the $\mu = 1.8$ case of Fig. 6, we reduce R to 10, where the single-packet OLA broadcasts take 10 hops (i.e., $M_0 = 10$). As before, the numerical results in Fig. 7 are obtained with $M = M_0 - 1 = 9$ as the minimum requirement for spatial pipelining. As shown in the figure, eight of the ten packets stop propagating in the middle of the network, which is much worse than the ring expansion case. The reason is that the OLAs transmitting the leading and following packets are more balanced in size and not so far from each other, causing significant interference in both directions.

This example results show that when $\alpha = 2$, packet loss happens even with ten packets and the marginal packet insertion period of $M = M_0 - 1$. Therefore, it is not possible to improve the broadcast throughput by spatial pipelining. Rather, it hurts the broadcast throughput by causing the side effects of the intra-flow interference such as degraded hop-distances and packet loss. Also, this overhead of spatial pipelining would become more significant for faster insertion rates with $M < M_0 - 1$ or more packets.

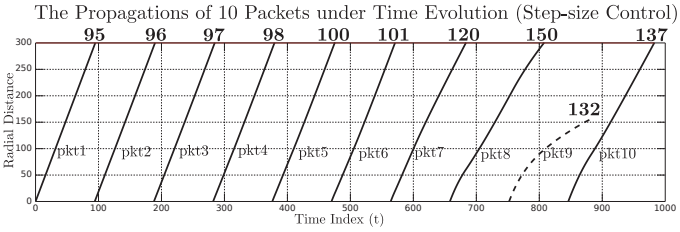

Fig. 8. The time evolution of distances with step-size control, when M=95, M_0=94, and R=300.

B. Step-size Control

Because the large size of the OLAs of the first packet can be blamed for shortening the second-packet hop-distances, we wondered if constraining OLA sizes would help the situation. It is straightforward to do power control as a function of hop count, to make OLA outer radii equally spaced. This "*step-size control*" approach was proposed in [16] for the purpose of regulating OLA sizes on the route reply phase of an OLA-based reactive routing scheme. In the single-packet OLA broadcasts, we can keep the same step-size of $\sqrt{(P_s/\tau)} = r_k - r_{k-1}$ for $k = 1, 2,$ ... by setting the relay transmission power at kth OLA to

$$P_r(k) = \frac{\tau}{\pi\rho \ln\left(\frac{4k}{2k+1}\right)}, \tag{25}$$

which is readily derived by the OLA boundary condition that $r_k = \sqrt{(P_s/\tau)}k$.

This equal step-size control technique is useful to suppress the intra-flow interference by avoiding the ring expansion problem. Fig. 8 shows the numerical results of the OLA broadcast with ten packets following the step-size control power adaptation, where the parameters are same to the numerical analysis in Fig. 6. However, because of the reduced total transmit power by the step-size control, the single-packet OLA broadcasts take $M_0 = 95$ hops, so we use one less packet insertion period of $M = 94$ for the pipelining. Compared to the results in Fig. 6, the impact of the pipelining is smaller in the step-size controlled network, which shows the packet loss of the ninth packet, even though the transmit power level of each relay is decreasing with hop index, to avoid the ring expansion. However, as in the previous fixed relay power examples, the step-size of each packet, which is indicated by the instantaneous slope of the curve, decreases from the first to the eighth packets. It can be also observed by the increasing total hop counts of the packets and the gradual slope variation in Fig. 8. Thus, the step-size of the ninth packet is being suppressed to tiny levels, and it stops propagating at the 132th hop.

V. Numerical Results with the Finite Network for Higher Path Loss Exponents ($\alpha > 2$)

For the finite disk networks, we showed numerically that the pipelined OLA broadcasts always degrade the broadcast

throughput for $\alpha = 2$, because of the significant co-channel interference and packet loss by the pipelining. On the other hand, through the theoretical analysis assuming even the infinite-size network in Section III, we showed that we can do spatial pipelining, when path attenuation is higher (i.e., $\alpha > 2$). For this reason, in this section, we investigate the broadcast throughput improvement by the spatial pipelining in finite networks for $\alpha > 2$. In contrast to the infinite disk network, the number of interfering OLAs in a finite network is bounded by the size of the network, since the preceding packets finish propagation once they reach the edge.

Because spatial pipelining is feasible, now our interest is to find the minimum packet insertion period, $M_{R,opt}$, that does not cause packet loss, where R is a finite radius. Finding $M_{R,opt}$ requires numerical calculations of the OLA boundaries $r_{(i;k)}$ for the all packet indices i and levels k at each time unit. We find the $M_{R,opt}$ by exhaustive search, testing whether there is packet loss for different M starting from 3. In Section V-A, we first observe the propagation patterns of the pipelined OLA broadcasts with a 20-packet example, Then, Section V-B and V-C provide the numerically computed $M_{R,opt}$ over the different system parameters α, τ, and $\overline{P}_r$.

A. Twenty-Packet Example in the Finite Disk Network

The following numerical results show the propagation patterns for $\alpha = 2.5$ and 4 using the minimum packet insertion periods $M_{R,opt}$ found by the exhaustive searches. Fig. 9 shows the numerical results of twenty-packet OLA broadcast with $\alpha = 2.5$, $M = M_{R,opt} = 6$, $\overline{P}_r = 30$ ($\mu \approx 1.0107$), $P_s = 30$, and $\tau = 1$, where the radius of the network $R = 68000$. For the single (or non-pipelined) packet OLA broadcast, it takes 50 hops to reach the network edge (i.e., $M_0 = 50$). The figure displays the traces of the twenty packets on the graph of time versus radial propagation distance. The numbers above the curves on the top of the graph mean the final hop counts of the 20 packets to reach the network edge.

The key observation in Fig. 9 is that there is no packet loss, even though the propagation speeds become slower as the packet index increases by pipelining with $M_{R,opt} = 6$. Other observations include that the first packet shows the least impact with the final hop count of 51, which is just one hop count larger than the single-packet case M_0, because the first packet grows fast while it does not undergo intra-flow interference until the second packet is inserted. On the other hand, the final hop counts of the next 19 packets are much bigger, because the network is being filled with pipelined co-channel packets. Especially, Packets 2 to 10 have significantly large final hop counts, because the interference of Packet 1 dominates other interference and gives long-lasting impacts to the packets. On the other hand, after this transition, Packets 11 to 18 show quite stable propagation patterns without a sudden change in the slopes, which gives similar final hop counts. On the other hand, the last two packets (Packets 19 and 20) are relatively unstable, because Packet 20 does not have following packets, which is a favorable propagation environment. For that reason, Packet 20 propagates rapidly until it approaches very close to Packet 19. Then, the two packets interfere with each other and become slower.

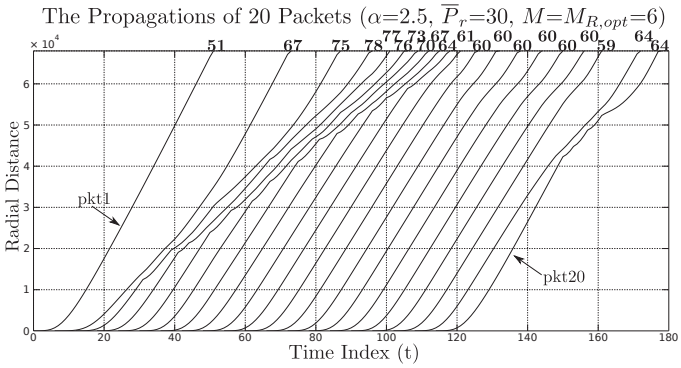

Fig. 9. Numerical results with twenty packets for $\alpha = 2.5$, when $M = M_{R,opt} = 6$, $M_0 = 50$, and $R = 68000$.

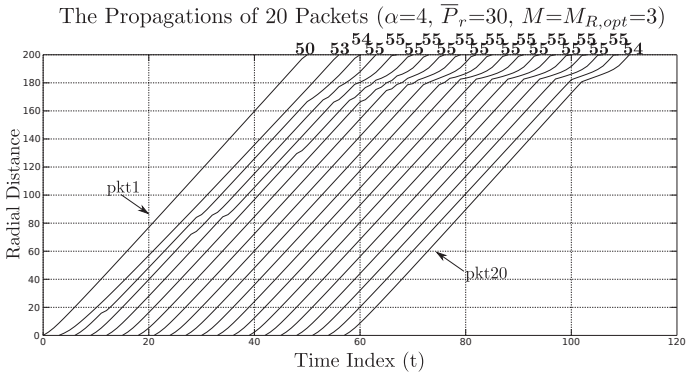

Fig. 10. Numerical results with twenty packets for $\alpha = 4$, when $M = M_{R,opt} = 3$, $M_0 = 50$, and $R = 200$.

Fig. 10 shows the numerical results of $\alpha = 4$ with $R = 200$, which is selected to obtain the same $M_0 = 50$ as the previous case. Also, except the disk size R, the other parameters are kept to be the same as Fig. 9 (i.e., $\overline{P}_r = 30$, $P_s = 30$, and $\tau = 1$). The exhaustive search gives $M_{R,opt} = 3$ for the given parameters, which is also the minimum of M under the half-duplex system assumption. As the previous example in Fig. 9, none of the twenty pipelined packets quit propagating in the middle of the network. Compared to Fig. 9, the slopes in Fig. 10 are smaller considering the different vertical axis scale, because the path attenuation is larger. However, the propagation patterns of the packets in Fig. 10 are more stable, and the slopes are less different than $\alpha = 2.5$ case in Fig. 9. These properties are because the higher path attenuation allows better spatial efficiency and less influence from the more distant co-channel interferers. For example, the throughput improvements by spatial pipelining in Figs. 9 and 10 compared to the non-spatial pipelining cases (the ratios of $M_0/M_{R,opt}$) are 50/6 ($\approx$8.33) and 50/4 (=12.5), which correspond to α of 2.5 and 4, respectively. Therefore, we can conclude that higher path attenuation allows higher throughput improvement by spatial pipelining from the non-spatial pipelining strategy.

Another interesting observation is that the slopes of Packet 3 to 20 vary significant around the edge $R = 180$, caused by the escape of the very preceding packet from the network. For example, after when Packet 3 reaches the edge, Packet 4 is suddenly accelerated, which makes the transmitting OLA size bigger. However, this sharp increase in Packet 4 works as a

severe increase in interference to Packet 5, which degrades the propagation speed of Packet 5. For this reason, the following packets after Packet 5 sequentially undergo de-acceleration. Therefore, the packets propagate slower as they approach the network edge, but they suddenly leap forward after when the very preceding packet finishes the propagation. We observe this behavior with different network sizes R. Even though the slopes are not dramatically changing, we can see a similar behaviors partially in Fig. 9.

We note that if the network size R increases, $M_{R,opt}$ is likely to increase because the network would accommodate more number of co-channel packets, which would cause higher intra-flow interference. As a result, in general $M_{R,opt}$ in the finite network is much smaller than the bound $\hat{M}_{I,opt}$ derived for the infinite network in Section III-C. For example, $M_{R,opt}$ for $\alpha = 2.5$ in Fig. 9 is six, while the corresponding $\hat{M}_{I,opt}$ in Table II is 2448. Also, when $\alpha = 4$, $M_{R,opt}$ in Fig. 10 is three, and $\hat{M}_{opt}$ in Table II is eight. The gap between $M_{R,opt}$ and $\hat{M}_{I,opt}$ is bigger for lower $\alpha = 2.5$, because the interfering OLA areas are inflated in $\mathbf{SINR}_{LB}$ by integrating to infinity. However, in particular for large α (e.g., $\alpha \approx 4$), $\hat{M}_{I,opt}$ can be helpful to limit the range of the exhaustive search for $M_{R,opt}$ by serving as an upper bound.

B. Impacts of α and $\overline{P}_r$ on $M_{R,opt}$

In this section, we test the effects of the path loss exponent α and the relay transmission power $\overline{P}_r$ on the optimal packet insertion period $M_{R,opt}$. Fig. 11 shows the numerical results with 20 packets, $\tau = 10$ and $M_0 = 50$ to compare the efficiency of the spatial pipelining (i.e., R changes depending on the parameters). In the figure, the horizontal axis indicates $\alpha = 2.5$, 3, 3.5, and 4, while the vertical axis indicates $M_{R,opt}$ obtained by the exhaustive search. Also, the solid and dotted lines represent $M_{R,opt}$ with $\overline{P}_r = P_s = 100$ and 400, respectively.

The both lines are decreasing as α increases, which means we can achieve more efficient spatial reuse with the increase in the broadcast throughput by a factor of $\frac{\eta_{R,opt}}{\eta_{M_0}} = \frac{M_0}{M_{R,opt}}$ for higher path attenuation. That is because the co-channel interference becomes less significant as α increases, which is also identical to the theoretical analysis assuming the infinite network in Section III-C2. On the other hand, if looking at the heights of the two graphs on the same α, the dotted line corresponding to $\overline{P}_r = 400$ is always under the solid line, which represents $\overline{P}_r = 100$. In other words, the spatial reuse efficiency for higher relay transmission power is better. The reasons is again the relative distance of the signal source OLA and the co-channel interfering OLAs. To be specific, as $\overline{P}_r$ increases, the resulting SINR also increases, since the signal power increase level is greater than the interference increase level even though both are growing. Also, we note that the height gap between the two graphs is the largest at $\alpha = 2.5$, which indicates the low α case is more vulnerable to the drop in $\overline{P}_r$.

C. Impacts of τ on $M_{R,opt}$

The final numerical results present how $M_{R,opt}$ changes under the decoding threshold $\tau = 5$, 10, 15, and 20 with

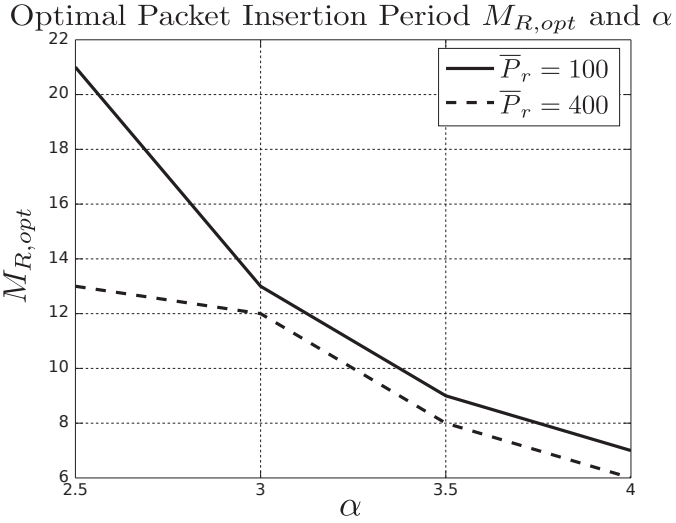

Fig. 11. Numerical results for the different path loss exponents $\alpha = \{2.5, 3, 3.5, 4\}$, when $M_0 = 50$, $\tau = 10$, and $\overline{P}_r = P_s = \{100, 400\}$.

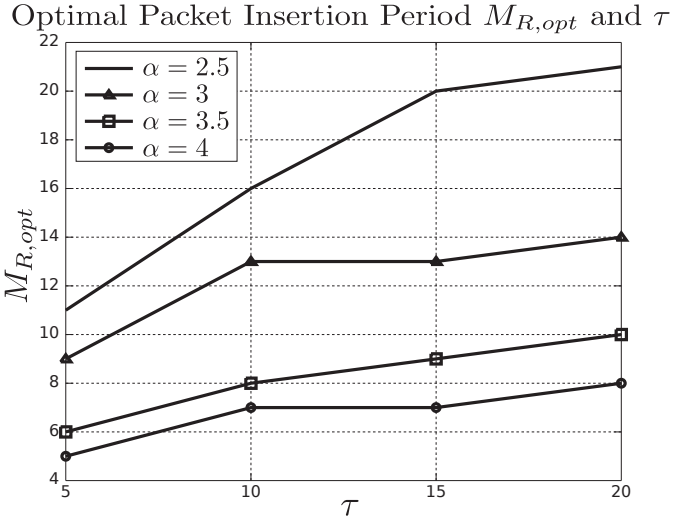

Fig. 12. Numerical results for the different decoding thresholds $\tau = \{5, 10, 15, 20\}$, when $\alpha = \{2.5, 3, 3.5, 4\}$, $M_0 = 50$, and $\overline{P}_r = P_s = 300$.

20 packets, $\overline{P}_r = P_s = 300$ and the radii R are chosen with $M_0 = 50$ to compare the efficiency of the spatial pipelining as the previous comparison. Fig. 12 shows the numerical results by the exhaustive search with the x-axis of τ and the y-axis of $M_{R,opt}$, where the different lines indicate the different α: the solid line without marker (2.5), the triangle-marker line (3), the square-marker line (3.5), and the circle-marker line (4). All the four lines show the increasing behavior (or keep the same level) $M_{R,opt}$ of as τ increases. This pattern results from a more demanding SINR condition as τ grows, which limits the interference levels.

If comparing the heights of the four curves, the lower path-loss exponent gives higher $M_{R,opt}$ for the same τ. In other words, $\alpha = 2.5$ shows the highest $M_{R,opt}$, and $\alpha = 4$ gives the lowest $M_{R,opt}$. That is because the higher α gives more significant improvement of the throughput by spatial pipelining as shown by the previous numerical results in Section V-B, since the impact of the intra-flow interference decreases as α grows, which is consistent with the analytical

result in Section III-C2. Moreover, the curve with the higher α shows more significant increases compared to the curve with the lower α, as τ increases. For example, as τ increases, the solid lines with no marker and the triangle-marker, which indicate $\alpha = 2$ and 2.5 respectively, show more increases of $M_{R,opt}$ than than the solid lines with the square- and circle markers, which represent $\alpha = 3.5$ and 4, respectively. That is because higher path attenuation (i.e., higher α) makes the sensitivity to τ smaller. This tendency is consistent with the infinite disk case based on the observation of $q(\alpha) \approx \hat{M}^*_{I,opt}$ defined in Section III-C2, which is an approximation of the finite network with very large R. For example, $\frac{\partial q}{\partial \tau}$ in (23), which indicates the sensitivity of $\hat{M}^*_{I,opt}$ to τ, is 20480, 32, 3.77834, and 1.26491 for $\alpha = 2.5$, 3, 3.5, and 4, when $\tau = 5$. Similarly, in Fig. 5 in Section III-C2, the height gaps of the three curves corresponding to $\tau = 1$, 10, and 100, which also indicate the sensitivity of $\hat{M}^*_{I,opt}$ to τ, are wider for smaller α.

However, the decreases in $M_{R,opt}$ under the change in τ is much less significant compared to $\hat{M}^*_{I,opt}$. For example, the $M_{R,opt}$ curves with $\alpha = 3$ and 4 do not change, when τ increases from 10 to 15. That is because the network size is finite, which limits the number of co-channel packets in the network, while $\hat{M}^*_{I,opt}$ assuming the infinite network is derived based on the highly inflated co-channel interference $\mathbf{I}$ in (18) than its actual value. Moreover, because $M_{R,opt}$ must be a positive integer, if the increase of τ is not significant enough, $M_{R,opt}$ does not change as the two cases (e.g., the curves with $\alpha = 3$ and 4, when τ increases from 10 to 15) shown in Fig. 12.

The decoding threshold τ depends on other various parameters (e.g., modulation order, packet size, and coding scheme) that change the data rate with non-trivial relationships. In this study, we limit our scope to the packet-level analysis as in [23] with the assumption that the parameters deciding τ is fixed for a certain system.

VI. Conclusion

In this paper, we study the impact of the intra-flow interference on throughput in OLA broadcasts using the continuum and deterministic channel assumptions, which model the high node density situation. For the infinite disk network, we prove that the intra-flow interference of multiple OLA broadcasts discourages spatial reuse for free space path loss exponent $\alpha = 2$, because any co-channel pipelining causes shorter step sizes that greatly delay the second packet, and the further insertion of packets causes packet loss. On the other hand, for higher path attenuation with $\alpha > 2$, we theoretically show that the spatial pipelining is feasible and derive the lower bound of the broadcast throughput.

Numerical results with the finite network sizes confirm the theoretical analysis that spatial pipelining hurts the broadcast throughput for $\alpha = 2$ by causing packet loss, while it improves the throughput and none of packets are lost when $\alpha > 2$, by taking advantage of spatial pipelining, which becomes more efficient as α increases. Therefore, the results indicate that the multiple-packet transmission strategy for OLAs should be determined based on the path attenuation. When $\alpha = 2$, we suggest the best strategy is to wait to insert a packet until after the preceding co-channel packet has reached the edge of the network. On the other hand, if $\alpha > 2$, the broadcast throughput can be improved by the spatial pipelining, which verifies that OLA broadcasts can be an effective solution for multiple-packet transmissions in the high path attenuation environments. Lastly, this paper shows the impact of the different system parameters on the optimal packet insertion period (i.e., the optimal broadcast throughput), which has the same trends both in the theoretical analysis in the infinite disk network and the numerical results in the finite disk network. Potential extensions of this paper include addressing a wider scenario with low diversity orders and low node densities.

References

[1] B. Williams and T. Camp, "Comparison of broadcasting techniques for mobile ad hoc networks," in *Proc. ACM MobiHoc*, pp. 194–205, 2002.

[2] S.-Y. Ni, Y.-C. Tseng, Y.-S. Chen, and J.-P. Sheu, "The broadcast storm problem in a mobile ad hoc network," in *Proc. ACM/IEEE MobiCom*, pp. 151–162, 1999.

[3] Q. Zhang and D. Agrawal, "Dynamic probabilistic broadcasting in mobile ad hoc networks," in *Proc. IEEE VTC*, vol. 5, pp. 2860–2864, Oct. 2003.

[4] J. E. Wieselthier, G. D. Nguyen, and A. Ephremides, "Energy-efficient broadcast and multicast trees in wireless networks," *Mobile Netw. Applications*, vol. 7, pp. 481–492, 2002.

[5] A. Das, R. Marks, M. El-Sharkawi, P. Arabshahi, and A. Gray, "Minimum power broadcast trees for wireless networks: integer programming formulations," in *Proc. INFOCOM*, vol. 2, pp. 1001–1010, Mar. 2003.

[6] Q. Yang, L. Shen, and W. Xia, "Distributed probabilistic broadcasting for safety applications in vehicular ad hoc networks," in *Proc. Int. Conf. Wireless Commun. Signal Process.*, pp. 1–5, Nov. 2009.

[7] A. Ahizoune, A. Hafid, and R. Ben Ali, "A contention-free broadcast protocol for periodic safety messages in vehicular ad-hoc networks," in *Proc. IEEE Conf. Local Comput. Netw.*, pp. 48–55, Oct. 2010.

[8] J. Laneman and G. Wornell, "Distributed space-time-coded protocols for exploiting cooperative diversity in wireless networks," *IEEE Trans. Inf. Theory*, vol. 49, no. 10, pp. 2415–2425, Oct. 2003.

[9] J. Laneman, D. Tse, and G. Wornell, "Cooperative diversity in wireless networks: efficient protocols and outage behavior," *IEEE Trans. Inf. Theory*, vol. 50, no. 12, pp. 3062–3080, Dec. 2004.

[10] I. Maric and R. Yates, "Cooperative multihop broadcast for wireless networks," *IEEE J. Sel. Areas Commun.*, vol. 22, no. 6, pp. 1080–1088, Aug. 2004.

[11] G. Jakllari, S. V. Krishnamurthy, M. Faloutsos, and P. V. Krishnamurthy, "On broadcasting with cooperative diversity in multi-hop wireless networks," *IEEE J. Sel. Areas Commun.*, vol. 25, no. 2, pp. 484–496, Feb. 2007.

[12] T. Halford and K. Chugg, "Barrage relay networks," in *Proc. Inf. Theory Applications Workshop*, pp. 1–8, Feb. 2010.

[13] A. Scaglione and Y.-W. Hong, "Opportunistic large arrays: Cooperative transmission in wireless multihop ad hoc networks to reach far distances," *IEEE Trans. Signal Process.*, vol. 51, no. 8, pp. 2082–2092, Aug. 2003.

[14] B. Sirkeci-Mergen, A. Scaglione, and G. Mergen, "Asymptotic analysis of multistage cooperative broadcast in wireless networks," *IEEE Trans. Inf. Theory*, vol. 52, no. 6, pp. 2531–2550, June 2006, corrected version: http://crisp.ece.cornell.edu/papers/BirsenITTran2006.pdf.

[15] Y. J. Chang, H. Jung, and M. A. Ingram, "Demonstration of an OLA-based cooperative routing protocol in an indoor environment," in *Proc. IEEE European Wireless*, pp. 1–8, Apr. 2011.

[16] L. Thanayankizil, A. Kailas, and M. A. Ingram, "Routing for wireless sensor networks with an opportunistic large array (OLA) physical layer," *Ad Hoc Sensor Wireless Netw.*, vol. 8, no. 1-2, pp. 79–117, 2009.

[17] L. Thanayankizil and M. Ingram, "Reactive routing for multi-hop dynamic ad hoc networks based on opportunistic large arrays," in *Proc. IEEE GLOBECOM*, pp. 1–6, 2008.

[18] L. Thanayankizil, A. Kailas, and M. A. Ingram, "Opportunistic large array concentric routing algorithm (OLACRA) for upstream routing in wireless sensor networks," *Ad Hoc Netw.*, vol. 8, no. 1-2, pp. 79–117, 2011.

[19] T. Halford, T. Courtade, and K. Turck, "The user capacity of barrage relay networks," in *Proc. IEEE MILCOM*, pp. 1–6, 2012.

[20] B. Sirkeci-Mergen and M. Gastpar, "On the broadcast capacity of wireless networks with cooperative relays," *IEEE Trans. Inf. Theory*, vol. 56, no. 8, pp. 3847–3861, Aug. 2010.

[21] H. Jung and M. A. Ingram, "Analysis of spatial pipelining in opportunistic large array broadcasts," in *Proc. IEEE MILCOM*, pp. 991–996, Nov. 2011.

[22] M.-K. Oh, X. Ma, G. Giannakis, and D.-J. Park, "Cooperative synchronization and channel estimation in wireless sensor networks," in *Proc. IEEE Conf. Signals, Syst. Comput. (ASILOMAR)*, vol. 1, pp. 238–242, Nov. 2003.

[23] A. Bader and E. Ekici, "Performance optimization of interference-limited multihop networks," *IEEE/ACM Trans. Netw.*, vol. 16, no. 5, pp. 1147–1160, Oct. 2008.

[24] B. Sirkeci-Mersen and A. Scaglione, "A continuum approach to dense wireless networks with cooperation," in *Proc. INFOCOM*, vol. 4, pp. 2755–2763, Mar. 2005.

[25] J. Proakis, *Digital Communications*. McGraw-Hill, 2000.

[26] A. Kailas and M. A. Ingram, "Alternating opportunistic large arrays in broadcasting for network lifetime extension," *IEEE Trans. Wireless Commun.*, vol. 8, no. 6, pp. 2831–2835, 2009.

[27] ——, "Analysis of a simple recruiting method for cooperative routes and strip networks," *IEEE Trans. Wireless Commun.*, vol. 9, no. 8, pp. 2415–2419, Aug. 2010.

[28] G. Jakllari, S. V. Krishnamurthy, M. Faloutsos, P. V. Krishnamurthy, and O. Ercetin, "A cross-layer framework for exploiting virtual MISO links in mobile ad hoc networks," *IEEE Trans. Mobile Comput.*, vol. 6, no. 6, pp. 579–594, June 2007.

[29] S. Lakshmanan and R. Sivakumar, "Diversity routing for multi-hop wireless networks with cooperative transmissions," in *Proc. IEEE SECON*, pp. 1–9, June 2009.

[30] J. W. Jung and M. A. Ingram, "Residual-energy activated cooperative transmission (REACT) to avoid the energy hole," in *Proc. IEEE ICC*, June 2010.

[31] B. Bash, D. Goeckel, and D. Towsley, "Clustering in cooperative networks," in *Proc. IEEE INFOCOM 2011*, pp. 486–490, Apr. 2011.

[32] H. Jung and M. A. Ingram, "SNR penalty from the path-loss disparity in virtual multiple-input-single-output (VMISO) link," in *Proc. IEEE ICC*, June 2013.

[33] G. L. Stuber, *Principles of Mobile Communications*, 2nd ed. Kluwer Academic Publishers, 2000.

[34] A. Kailas, L. Thanayankizil, and M. A. Ingram, "A simple cooperative transmission protocol for energy-efficient broadcasting over multi-hop wireless networks," *J. Commun. Netw.*, vol. 10, no. 2, pp. 213–220, 2008.

[35] A. Kailas, "On the performance of alternating concurrent cooperative transmissions in the high path-loss attenuation regime," *Int. J. Netw. Protocols Algorithms*, vol. 4, no. 2, pp. 68–81, 2012.

[36] M. Garetto, T. Salonidis, and E. Knightly, "Modeling per-flow throughput and capturing starvation in CSMA multi-hop wireless networks," *IEEE/ACM Trans. Netw.*, vol. 16, no. 4, pp. 864–877, Aug. 2008.

[37] Y. J. Chang, M. A. Ingram, and S. Frazier, "Cluster transmission time synchronization for cooperative transmission using software defined radio," in *Proc. IEEE ICC*, June 2010.

[38] T. Rappaport, *Wireless Communications: Principles and Practice*. Prentice Hall PTR, 2001.

Haejoon Jung received the B.S. degree from Yonsei University, Seoul, South Korea in 2008. He is currently pursuing his Ph.D. degree in Electrical and Computer Engineering at the Georgia Institute of Technology (Georgia Tech), Atlanta, USA. He has been working in the Smart Antenna Research Laboratory (SARL) as a graduate research assistant. His research interests include wireless network and communication system, focusing on cooperative communications. He also worked for Samsung Electronics (Kihueng, South Korea) as a summer intern in 2009 and 2011.

Mary Ann Weitnauer (formerly Mary Ann Ingram) received the B.E.E. and Ph.D. degrees from the Georgia Institute of Technology (Georgia Tech), Atlanta, USA, in 1983 and 1989, respectively. In 1989, she joined the faculty of the School of Electrical and Computer Engineering at Georgia Tech, where she is currently Professor. Her early research areas were optical communications and radar systems. In 1997, she established the Smart Antenna Research Laboratory (SARL) at Georgia Tech, which applies real and virtual array antennas to wireless networks and radar systems. She held the Georgia Tech ADVANCE Professorship for the College of Engineering from 2006-2012. She was a Visiting Professor at Aalborg University, Aalborg, Denmark in the summers of 2006-2008 and at Idaho National Labs in 2010. The SARL performs system analysis and design, channel measurement, and prototyping relating primarily to wireless local area, ad hoc and sensor networks, with focus on the lower three layers of the protocol stack. SARL has also recently developed signal processing algorithms for impulse radio ultrawideband (IR-UWB) for non-contact vital signs measurement. Dr. Weitnauer has authored or co-authored over 160 refereed journal and conference papers, including four conference papers that have won Best Paper awards. She served as a Guest Editor for the EURASIP Special Issue on Cross-Layered Design for Physical/MAC/Link layers in Wireless Systems in 2007 and Co-Chair for America for the IEEE Wireless VITAE Conference in 2009. She was an associate editor for the IEEE TRANSACTIONS ON MOBILE COMPUTING from 2009-2012. Dr. Weitnauer is a Senior Member of the IEEE.